Widely tunable single-mode slot waveguide quantum cascade laser array

Jinghao Li, Fangyuan Sun, Yuhao Jin, Yun Da Chua, Kian Hua Tan, Satrio Wicaksono, Carlo Sirtori, Soon Fatt Yoon, Qi Jie Wang, Yun Da Chua, et al.

HAL Id: hal-03519466

https://hal.sorbonne-universite.fr/hal-03519466v1

Submitted on 10 Jan 2022

Widely tunable single-mode slot waveguide quantum cascade laser array

JINGHAO LI,[1] **FANGYUAN SUN,**[1] **YUHAO JIN,**[1] **YUN DA CHUA,**[1] **KIAN HUA TAN,**[2] **SATRIO WICAKSONO,**[2] **CARLO SIRTORI,**[1,3] **SOON FATT YOON,**[2] **AND QI JIE WANG**[1,4,*]

[1]*Centre for OptoElectronics and Biophotonics, School of Electrical and Electronic Engineering, Nanyang Technological University, Singapore 639798, Singapore*

[2]*Department of Electrical and Computer Engineering, National University of Singapore, Singapore 117583, Singapore*

[3]*Laboratoire de Physique de l'Ecole Normale Supérieure, ENS, Universite PSL, CNRS, Sorbonne Universite, Universite de Paris, 24 Rue Lhomond, 75005 Paris, France*

[4]*Centre for Disruptive Photonic Technologies, Division of Physics and Applied Physics, School of Physical and Mathematical Sciences, Nanyang Technological University, Singapore*

[*]*qjwang@ntu.edu.sg*

Abstract: We report designs and experimental demonstrations of a widely tunable single-mode quantum cascade laser array based on slot waveguide structures in the mid-infrared region. The laser array device realized a continuous tuning range of 71 cm^{-1} from 9.66 μm to 10.37 μm at 300 K only using the current tuning without any external heatsink temperature adjustments, in good agreement with the design. Stable single-mode operations free of undesired mode-hops have been obtained over the whole tuning range. Another slot waveguide QCL array with a 41 cm^{-1} continuous tuning range around 7.3 μm has also been realized with the same design principle, demonstrating the universal applicability of the array design. The broadly continuous tuning with simple processing makes the array device a suitable candidate for mid-infrared sensing and spectroscopy application.

1. Introduction

Single-mode tunable quantum cascade lasers (QCLs) with broad wavelength tuning range and narrow linewidth have become significant radiation sources for mid-infrared spectroscopy application, especially the multiple trace gas sensing with high sensitivity and high selectivity [1,2]. Such laser systems have already been demonstrated and commercialized by using external cavity QCLs (EC-QCLs) [3]. With optimized external cavity configurations, EC-QCLs can achieve single-mode wavelength selection over a wide gain bandwidth [4]. Nonetheless, the vibration-sensitive mechanical components compromise the repeatability and tuning speed of the system. To overcome these limitations, monolithic broadband tunable QCLs such as distributed-feedback (DFB) QCL arrays [5–7], superstructure distributed Bragg reflection (DBR) QCLs [8] and sampled grating distributed feedback (SG-DFB) QCL arrays [9,10] are investigated, which exhibit remarkable performances including high side mode suppression ratio (SMSR) and wide wavelength coverage. However, all of them require complicated fabrication processes, which increase the difficulty in their mass productions.

The proposal and realization of slot waveguide QCLs demonstrated the possibility to combine the simplified fabrication and broad single-mode tunability [11]. A slot waveguide QCL is composed of two electrically separate sections. By etching shallow slots into the top cladding of each section, the two sections act as reflectors providing two comb-like reflection spectra with different spacings between reflection peaks. The single-mode lasing happens when the peaks from two sections overlap. A minor refractive index variation of one section owe to the Joule

heating generated by DC current contributes to the overlap of another two peaks. As a result, a wide single-mode tuning can be achieved because of this Vernier effect mechanism [12–16]. Additionally, a continuous tuning operation can be conducted by simultaneously adjusting the refractive indexes of both sections with two independent DC currents. By optimizing the slot periods and number, a wide single-mode continuous tuning range of ∼ 42 cm^{-1} based on slot waveguide QCLs using pure current tuning under room temperature (RT=300 K) has been reported [17]. Nevertheless, broader tuning ranges and higher tuning resolutions are required in the real sensing applications. For the further extension of continuous tuning range with mode-hop free fine-tuning, the implementation of a set of slot QCLs in an array scheme becomes a promising option.

In this paper, we report the design and experimental development of a broadly and continuously tunable array formed by ten slot waveguide QCLs emitting at a center wavelength of ∼10 μm. For each laser, the slot dimension and number are optimized to form a shorter cavity than the one in Ref. [17] without degrading the SMSRs. Here different QCLs are designed to emit at distinct wavelength ranges, with the entire array showing a continuous tuning range of 71 cm^{-1} between 9.66 and 10.37 μm at room temperature, which is achieved exclusively with the tuning of currents. Compared to the previous work on the single slot QCL, the array device holds the advantage of stable single-mode tuning without any unpredictable mode-hops. Using the same array design principle, we also report another QCL array composed of five slot waveguide QCLs, which can be continuously tuned between 7.25 and 7.48 μm.

2. Device structure and design

The 10 μm QCL structure used in the present work is based on a 35-period lattice-matched In$_{0.53}$Ga$_{0.47}$As/In$_{0.52}$Al$_{0.48}$As bound-to-continuum active region design with high doping, as described in Ref. [18]. The wafer is grown by MBE on a conductive InP substrate starting from an InP layer ($n = 1 \times 10^{17}$cm^{-3}, 4 μm), followed by an InGaAs spacer ($n = 3 \times 10^{16}$cm^{-3}, 610 nm) and the active region. An upper InGaAs spacer same as the lower one is then grown symmetrically. The upper waveguide cladding consisting of two InP layers ($n = 1 \times 10^{17}$cm^{-3}, 3 μm and $n = 5 \times 10^{18}$cm^{-3}, 1 μm in sequence) exactly follows that. A highly doped 10-nm InP plasmon layer and a 20-nm InGaAs contact layer on top finally complete the growth.

The schematic structure of the ten-element slot waveguide QCL array is shown in Fig. 1(a). Each emitter of the array has a ridge waveguide structure with 24 μm width and 10 μm depth. The slots are etched on the ridge surface of front and back sections with different periods to introduce the Vernier effect between the reflections from the two sections. In the development of slot waveguide laser, the facet phase effect remains a non-negligible issue [11,19]. As discussed in Ref.11, The distance between facet and adjacent slot L_{pf} (L_{pb}) must be the integral multiple of the corresponding slot period to build a constructive interference between the reflections from the slots and facet. This requirement is difficult to fulfill due to the uncertainty of the facet cleavage position, which might lead to poor single-mode selectivity or unexpected mode hoping. To solve this problem, we electrically isolate the part between the facet and slots of each section, with a distance from facet to the last slot set as the double of the corresponding slot period, as presented in Fig. 1(c). This scheme allows us to adjust the refractive index of the isolated facet section $n_{eff-facet}$ by applying an additional DC current. In this way, we can keep the phase term of reflection from facet $exp\,[kn_{eff-facet}L_{pf}\,(L_{pb})]$ constant to maintain the constructive interference even though the L_{pf} (L_{pb}) deviates from the designed value.

The slot depth and number are the two key parameters affecting SMSRs, which must be optimized at the beginning [20,21]. In this work, the field reflection coefficient (r_s) and transmission coefficients (t_s) of a single slot at 10 μm with different slot depths are simulated using finite-difference time-domain (FDTD) method, as presented in Fig. 2(a). And the waveguide loss of back section α_b was calculated as ∼ 22 cm^{-1} by a linear least-squares fit to the measured
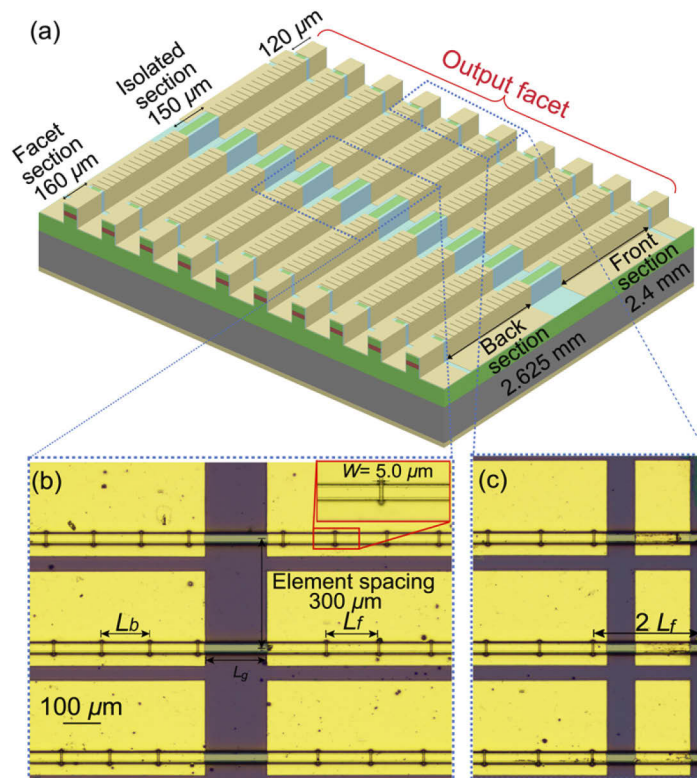
Fig. 1. (a) 3D schematic structure of a slot waveguide QCL array. (b) Microscopy image of the isolated region between two sections. The slot period of front (back) section is labelled as L_f (L_b). The spacing between the elements of array is 300 μm. The inset magnifies the image of one slot with a width of W=5 μm. (c) Microscopy image of the isolated facet section. The distance from facet to the last slot of each section is designed equal to the double of the slot period.

threshold current densities of Fabry-Perot (FP) cavity QCLs as a function of $1/L_{cavity}$. By using these results and the same procedure formulated in Ref.11, the reflection spectra with different slot depths and numbers were calculated. The loss differences between the dominant and side modes and the linewidths of the dominant peaks could be obtained from the spectra. The loss difference between the dominant and side modes can be used to represent the single-mode selectivity of a slot-waveguide laser [13]. With a larger loss difference, a higher SMSR could be acquired. Figure 2(b) describes how slot depth and number determine the loss difference. According to this simulated result, the loss difference generally increases when the slot number or slot depth increases because more feedbacks are provided by the slots. However, rising slot depth and number induce larger additional scattering loss, which impairs the power transmission through the cavity and thus the single-mode selectivity [20]. That is the reason why the 3.0 μm slot depth leads to a smaller loss difference than 2.8 μm when the slot number is large. Figure 2(c) presents the linewidths of reflection peaks with different slot depths and numbers. It is revealed that the linewidth drops and saturates quickly with increasing slot number. After the saturation, a smaller slot depth results in a narrower linewidth. It should be noticed that the free spectral range (FSR) of FP modes in our QCL cavity is around 0.25 cm^{-1}. To obtain a single FP mode selection, a linewidth of reflection peak =< 0.5 cm^{-1} is required. Therefore, slots with depth =< 2.4 μm and enough number are preferred. In conclusion, there is a trade-off between maximizing the

loss difference and minimizing the reflection peak linewidth when choosing slot depth. And increasing the slot number is an efficient method to realize a higher SMSR. Nevertheless, more slots make a longer cavity length raising the difficulty of device processing. Considering about
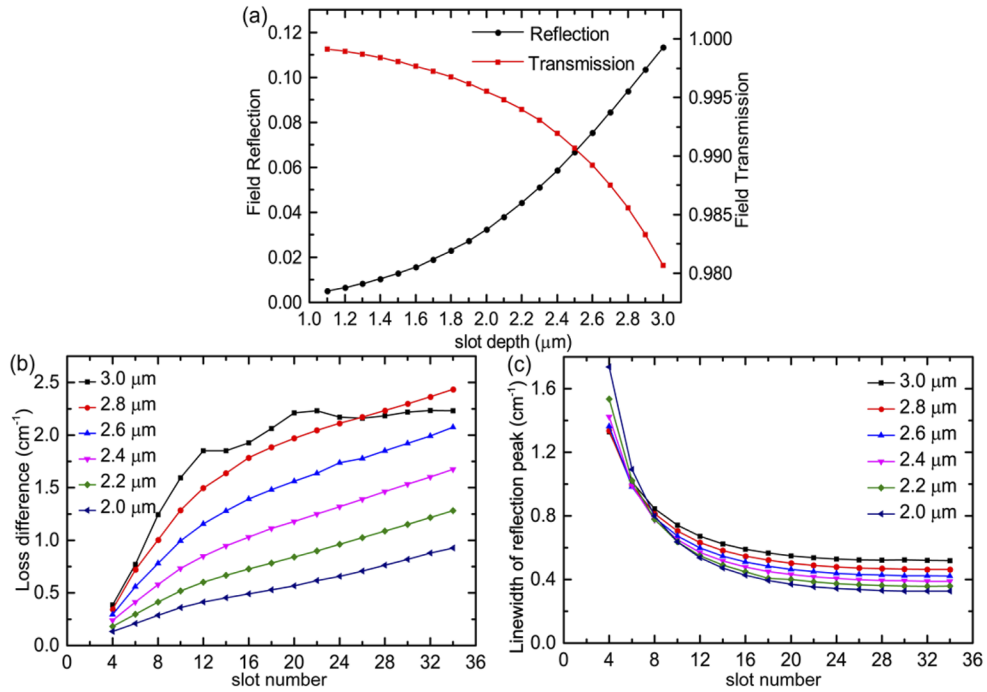
Fig. 2. (a) Field reflection and transmission coefficients of a single slot versus the slot depths. (b) Simulated loss difference between the dominant and side modes versus the slot number with various slot depths. The degradation of loss difference at 3.0 μm slot depth with the increase of the slot number arises from the large scattering loss induced by the deep slots. (c) Simulated linewidth of the reflection peak versus the slot number with various slot depths.
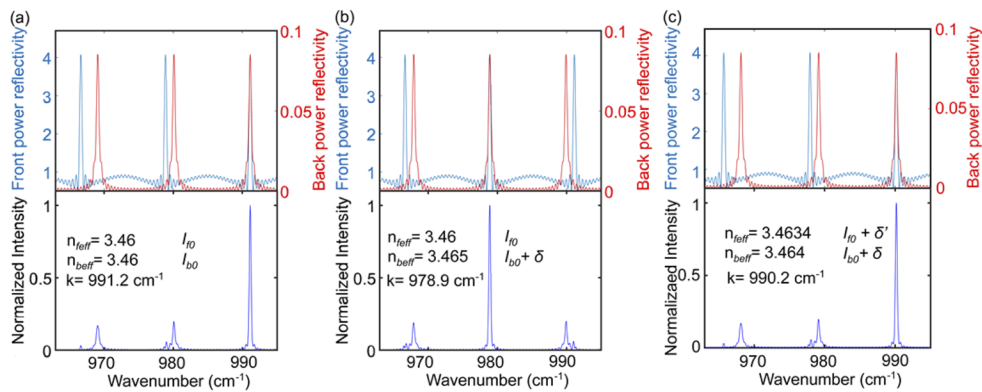
Fig. 3. Illustration of the tunability for QCL 1 by simulation. (a), (b) and (c) represent three conditions with different refractive indexes of the two sections induced by the two independent DC currents. Top: the power reflection spectra produced by front and back sections. Bottom: the corresponding total power reflection spectra showing the selected wavenumbers.
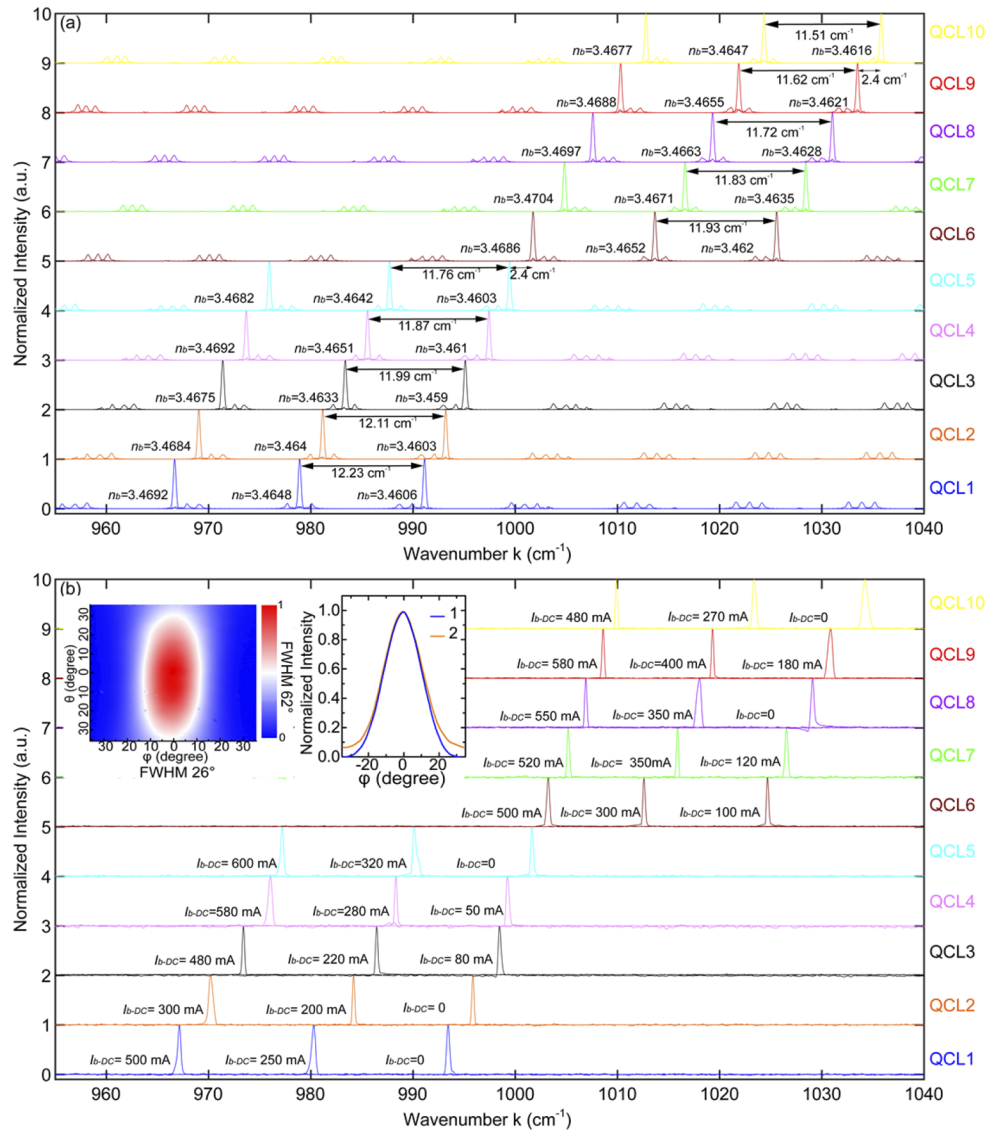
Fig. 4. (a) Simulated reflection spectra of supermodes from all the emitters of the slot waveguide QCL array. For each laser, the refractive index of the front section is assumed as 3.46 and three supermodes are shown with various refractive indexes of the back section. The spacing between the supermodes from different emitters is designed ~2.4 cm^{-1}. (b) Emission spectra of supermodes from all the emitters of the slot waveguide QCL array. For each laser, the front section was pumped by only pulse current and three supermodes working at different back section DC currents are shown, which is in good agreement with the simulated result above. The inset shows a typical single lobed 2D far-field pattern (left) and 1D far-field profile in-chip-plane (right) of our lasers. Nine of the elements except for QCL 2 exhibit a TM$_{00}$ mode with an in-plane far-field FWHM of ~26° as QCL 1 (blue curve). QCL 2 (orange curve) exhibits an in-plane far-field profile slightly contributed by higher-order lateral modes but still maintains a FWHM of ~26°.

all above analysis, the slots in this work are optimized with a depth of 2.4 μm and number of 22, which give a loss difference of $\sim 1.3\,\text{cm}^{-1}$ and a linewidth of reflection peak of $\sim 0.5\,\text{cm}^{-1}$.

The tunability of a slot waveguide QCL originates from a combination of the Vernier effect and continuous tuning. Fig. 3(a) and (b) illustrate the Vernier effect of QCL 1 with simulated reflection spectra. A slight refractive index variation ~ 0.005 of the back section can result in overlapped mode switching with large wavenumber spacing. In experiments, the local refractive index change of the back section could be induced by changing injected DC current to yield different supermodes lasing. The continuous tuning is carried out via adjusting the refractive indexes of both front and back sections. As described in Fig. 3(a) and (c), increasing the refractive indexes of both sections simultaneously with proper increments leads to a synchronous redshift of their reflection spectra. Consequently, the selected mode has a redshift from the given supermode.

Table 1. Design parameters of each emitter

| QCL	Period of front section L_f (μm)	Period of back section L_b (μm)	Slot grating order of front section M	Slot grating order of back section N	Wavenumber of designed supermode (cm^{-1})
1	118.1	131.2	81	90	991.2
			80	89	978.9
			79	88	996.7
2	119.3	132.4	82	91	993.3
			81	90	981.2
			80	89	969.0
3	120.5	133.6	83	92	995.4
			82	91	983.4
			81	90	971.4
4	121.7	134.7	84	93	997.4
			83	92	985.6
			82	91	973.7
5	122.9	135.9	85	94	999.5
			84	93	987.7
			83	92	975.9
6	121.1	132.3	86	94	1026.2
			85	93	1014.3
			84	92	1002.4
7	122.2	133.3	87	95	1028.8
			86	94	1017.0
			85	93	1005.2
8	123.3	134.4	88	96	1031.4
			87	95	1019.6
			86	94	1007.9
9	124.4	135.5	89	97	1033.9
			88	96	1022.2
			87	95	1010.6
10	125.5	136.6	90	98	1036.3
			89	97	1024.8
			88	96	1013.3

This process can be experimentally achieved by employing two independent DC currents to both sections. With the fine current adjustment, a very small tuning step can be realized. The continuous tuning around a supermode usually has a limited range $< 3\,\mathrm{cm}^{-1}$ because high DC currents cause a serious thermal effect that degrades the laser performance.

In order to make sure of a wide continuous tuning range free of gaps, the supermodes of each individual emitter need to be designed lasing at distinct wavelengths, and the spacing between the supermodes from different lasers should be sufficiently small so that any wavelengths within the designed range could be covered through the continuous tuning.

The supermode wavelength of a slot waveguide QCL can be expressed as [22]:

$$\lambda_{MN} = \frac{2n_{feff}L_f}{M} = \frac{2n_{beff}L_b}{N}. \tag{1}$$

where the n_{feff} (n_{beff}) is the effective refractive index of the front (back) section, L_f (L_b) is the slot period of the front (back) section and M (N) represents the slot grating order of front (back) sections. In this design, the effective refractive index unbiased is evaluated as ~ 3.46 by a two-dimensional waveguide simulation. By choosing proper grating orders and slot periods for QCL 1~10, the supermodes of all 10 lasers are simulated as Fig. 4(a), covering the range from 967 to $1036\,\mathrm{cm}^{-1}$. The design parameters of each laser are also listed in Table 1. Fig. 5(a) simulates typical continuous tuning spectra around a supermode with variable refractive indexes of both sections, which could fill up the tuning gap between supermodes as small as $\sim 2.4\,\mathrm{cm}^{-1}$. Therefore, a fully continuous tuning range around $965 \sim 1036\,\mathrm{cm}^{-1}$ could be predicted. The total length of the laser on our array is 5.455 mm, much shorter compared to the previous design (7.2 mm) in Ref.17.
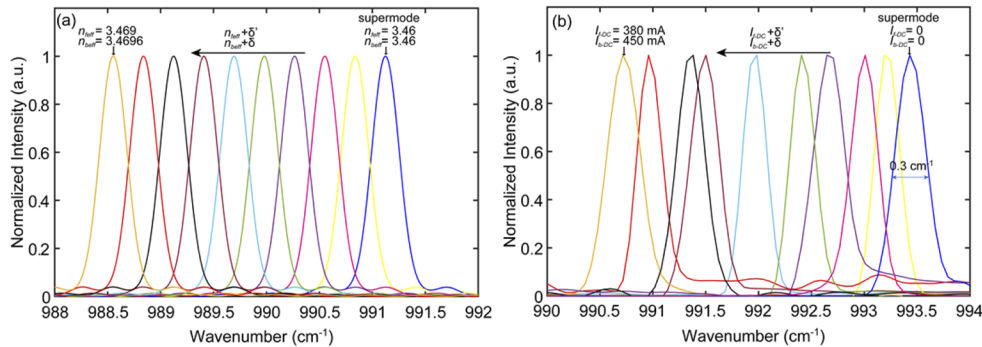
Fig. 5. (a) Simulated reflection spectra that illustrates a continuous tuning around a supermode of QCL 1 with variable refractive indexes of both sections. Different colors represent modes with different refractive indexes. (b) Emission spectra that illustrates a continuous tuning around a supermode of QCL 1 with two independent DC currents applied on both sections. Different colors represent modes with different currents. The average linewidth of the single-mode lasing peak is around $0.3\,\mathrm{cm}^{-1}$.

3. Array fabrication and characterization

The device processing started with defining the slot pattern on the surface of the diced wafer with a standard lithography process. After that, the slots were etched 2.4 μm deep into the top cladding with the inductively coupled plasma reactive ion etching (ICP-RIE) process. The ridge array with 24-μm width, spaced 300 μm apart, were defined by lithography aligned with the existing slot pattern. The ridges were then etched with ICP-RIE to 10-μm depth. Afterwards, the deposition of 500-nm SiO$_2$ was used to insulate the bottom and sidewall of ridges and a

Ti/Au top contact layer was formed with e-beam evaporation. The four sections of an individual laser and the different emitters were electrically separated through a gold wet etching with I_2/KI mixed solution. The isolated sample was thinned down to approximately 200 μm with Ti/Au back contact deposited. In the end, the device was cleaved to create laser facets and epilayer-side up bonded on a Cu heatsink with a thin indium layer. The electrical isolation resistances of the fabricated emitters between the front and back sections with zero bias were in the range from 250 to 300 Ω. The entire array chip is 3 mm by 5.455 mm in size.

All the characterizations of the as-cleaved device were conducted under room temperature. The temperature of the heatsink was controlled with a thermoelectrically cooled (TEC) stage regulated at 300 K. And for each emitter of the array, only the front section was pumped by a pulsed current (100 ns/10 kHz) and the output was collected from the facet of front section to ensure sufficient power collection. The Light-Current-Voltage (L-I-V) characteristics of the ten lasers were measured with a calibrated thermopile detector before the spectral characterization, as shown in Fig. 6. The threshold current densities of all ten elements were recorded in the range from 7.5 to 8.7 kA/cm^2, much higher than that ($\sim$ 5 kA/cm^2) of the pure FP cavity laser with a similar cavity length (2.5 mm), which is mainly owe to the strong free carrier loss of back section.
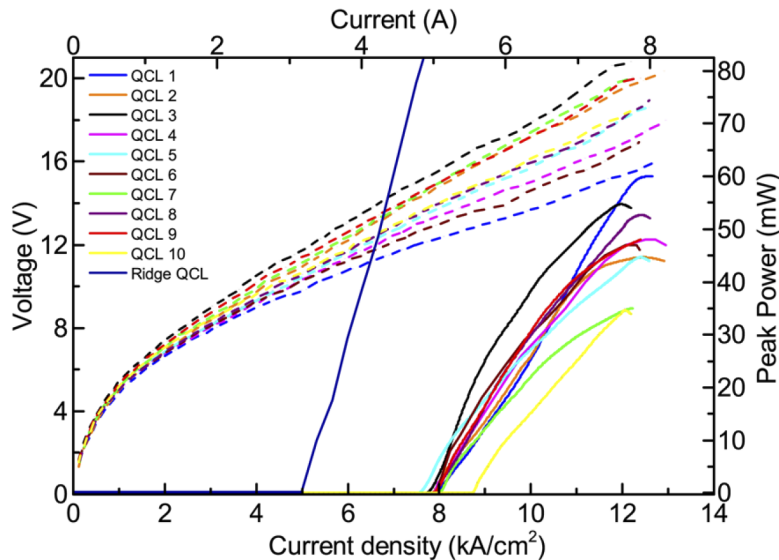
Fig. 6. Peak power and voltage versus current density curve for ten emitters of the slot array and the FP cavity laser with 2.5 mm length. The slot QCLs are pumped by only pulsed current (100 ns/10 kHz) into the front section without DC currents injected.

The spectral characterizations of the array were carried out by a Fourier Transform infrared spectroscopy (FTIR) system at a 0.2 cm^{-1} resolution with its internal HgCdTe detector. In the first step of the testing, we injected DC current I_{b-DC} from 0 to 600 mA into the back section of each laser, with the front section driven by only the pulsed current at 1.2 times of threshold value. The supermodes of each laser with different back section currents are plotted in Fig. 4(b). The ten QCLs operate at different wavelengths between 966 and 1035 cm^{-1} generally as designed. A minor deviation from the simulation result could be attributed to the refractive index evaluation error and the dispersion of semiconductor materials. The current tuning coefficient for back section dn_{beff}/dI_{b-DC} can be calculated as around 2.1$\times$10^{-5} mA^{-1} according to Fig. 4 (a) and (b), which is larger than the one reported in Ref.17 thanks to the shortened cavity. The coefficient for front section dn_{feff}/dI_{f-DC} is slightly smaller than dn_{eff}/dI_{b-DC} because of the slight difference between the sizes of the two sections. Besides, the beam qualities of all the emitters were also
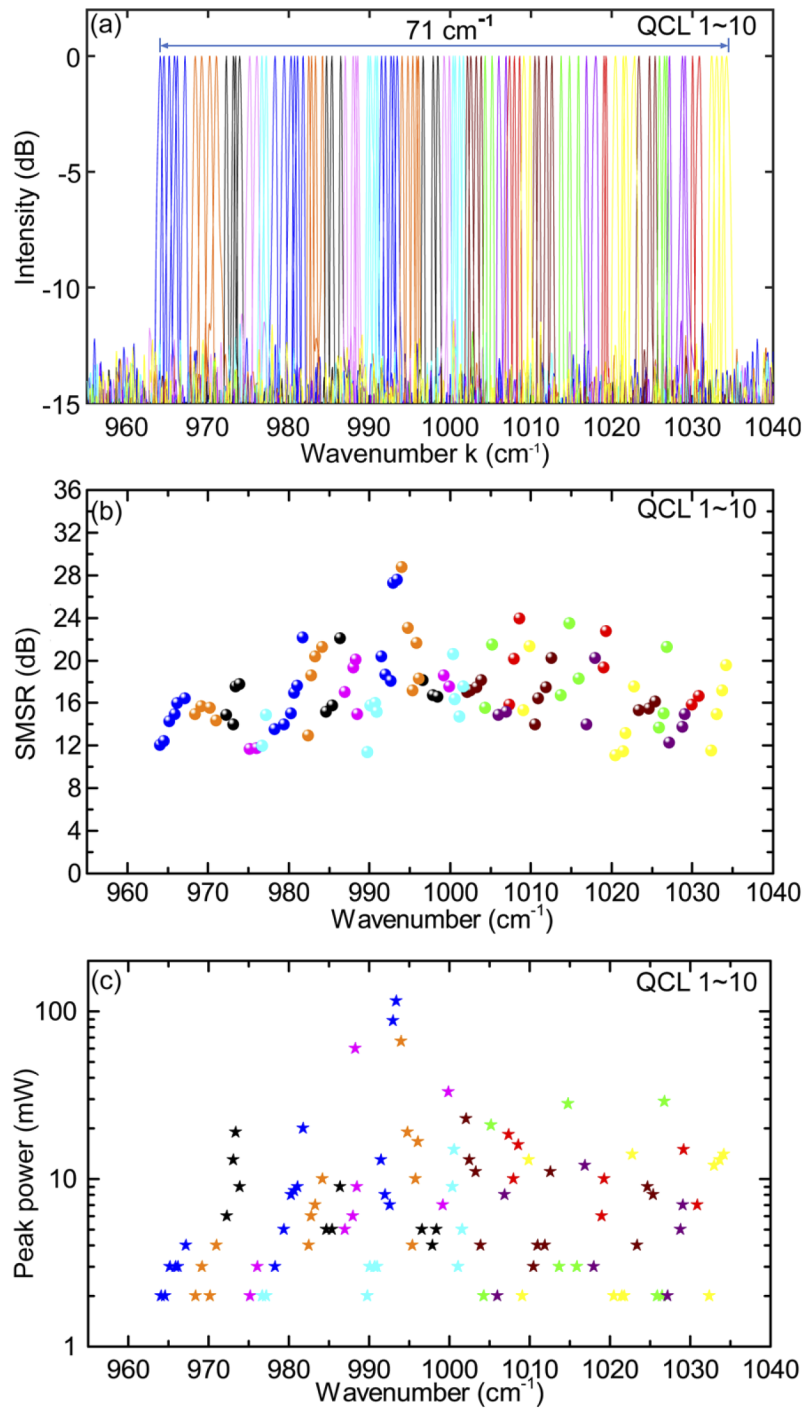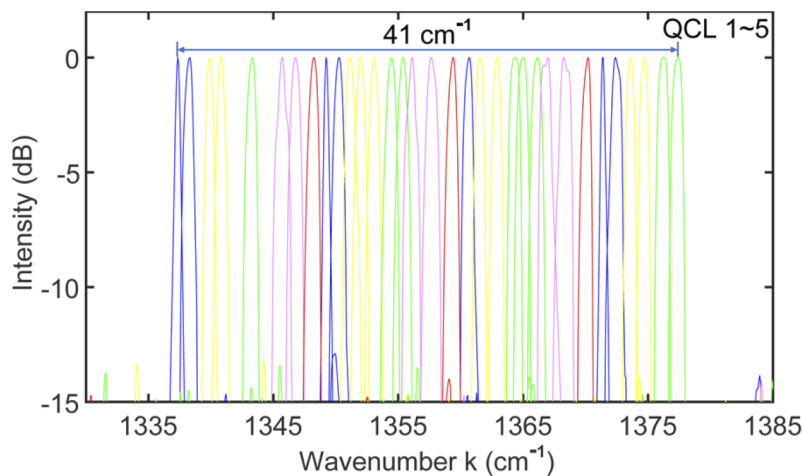
Fig. 7. (a) Single-mode tuning spectra of the 10-element slot waveguide QCL array showing a continuous tuning over 71 cm^{-1} around 10 μm. (b) The SMSRs of the modes within the continuous tuning range versus the wavenumber, most of which are >=15 dB. (c) The output peak powers of the modes within the continuous tuning range versus the wavenumber. Some of the modes show higher output powers compared to the maximum ones in Fig. 5 because the DC currents injected to back section provide more gain.

investigated by measuring the far-field distribution of the laser outputs under single longitudinal mode operations, as shown in the inset of Fig. 4(b). All the lasers exhibit a FWHM of in-plane far-field profile as ~26°.

The second step was to characterize the continuous tuning of the device. In this case, the front section of each laser was driven by a variable pulsed current (1.1~1.5 threshold value) combined with a DC current I_{f-DC} (from 0 to 400 mA) through bias-tee, while the back section was driven by the other DC current I_{b-DC} (from 0 to 1000 mA). Fig. 5(b) shows a typical experimental continuous tuning from a given supermode of QCL 1 with dual section DC current control. By varying I_{b-DC} from 0 to 450 mA (with 50 mA step) and supplying proper I_{f-DC} from 0 to 380 mA accordingly, a fine-tuning with a step ~ 0.3 cm^{-1} from 993.4 to 990.7 cm^{-1} was achieved, which could fully fill up the gap between supermodes. Applying such operating scheme to all the elements, a continuous tuning over 71 cm^{-1} (712 nm) from 964 to 1035 cm^{-1} (from 9.66 to 10.37 μm), which is 7.1% relative tuning range at center wavelength ~10 μm, was observed using our array as plotted in Fig. 7(a). To eliminate the undesirable mode-hops originating from the facet phase effect, the isolated facet section of each laser was also tuned with DC current from 0 to 50 mA. According to the characterization result, the slot QCL array provides a compact and predictable single-mode continuous tuning operation. Any emission wavelengths within the tuning range can be recalled by applying calibrated currents.

Figure 7(b) and (c) respectively show the SMSRs and maximum output peak powers of all the single modes presented in Fig. 7(a). Most lasing modes emitted by the array exhibit SMSRs of >=15 dB and peak powers from 2 to 110 mW. The relatively low SMSRs and output peak powers of some modes are partly ascribed to the thermal effect induced by the high DC current into the front section. Another reason for the limited SMSRs and output powers is that the gain profile based on a bound-to-continuum active region design is not sufficiently broad and flat [18], which enhances the mode competition between different frequencies. As a result, the multiple-mode operations are easy to be activated by high pumping currents. In our experiment, the pulsed currents were set variable below 1.5 threshold values.

Furthermore, we demonstrated another tunable slot waveguide array consisting of five emitters operating at a center wavelength of ~ 7.3 μm. The QCL wafer used is based on a bound-to-continuum active region design in Ref.4. The five-element array shows a continuous tuning range of 41 cm^{-1} (230 nm) from 1337 cm^{-1} to 1378 cm^{-1} (from 7.25 to 7.48 μm) with a SMSR of ~

Fig. 8. Experimental demonstration of single-mode tuning spectra of the 5-elemenmt slot waveguide QCL array showing a continuous tuning over 41 cm^{-1} around 7.3 μm.

15 dB as seen in Fig. 8, which certificates that the design principle for our slot waveguide QCL array could be commonly applied at different mid-infrared wavelength regions.

4. Conclusion

In summary, we presented both the design and experimental demonstration of a 10-element broadly tunable single-mode QCL array based on slot waveguide structures. Through the optimization of slot dimension and the design of array structure, a continuous tuning range from 965 to 1036 cm^{-1} was predicted. The fabricated array device realized a robust RT single-mode continuous tuning operation from 964 to 1035 cm^{-1} with an average SMSR of $\sim$ 15 dB, in good agreement with the designed result. The array successfully exhibits an extended continuous tuning range based on the single slot QCL. Due to the characteristic of mode-hop free tuning, the tuning of the array is in a controllable way that could be predicted by the design. Moreover, small spacing between the single modes was obtained through adjusting DC currents finely, which could increase the sensing resolution especially for the gases with narrow absorption peaks. Despite the limitation of low output powers compared to other single-mode tunable QCL platforms [23,24], the clear advantage of easy fabrication by using only standard lithography technique renders the slot waveguide QCL array an appropriate approach to the practical mid-infrared sensing and spectroscopy. In addition, our design principle of slot waveguide QCL array is universal, which is used to fabricate a device with a continuous tuning range of 41 cm^{-1} around 7.3 μm as well. In the future, by using the QCL design with optimized flat and broadband gain profile such as heterogeneous cascade active region design [4,10], a broader continuous tuning range could be possibly achieved with the slot waveguide QCL array.

Disclosures. The authors declare that there are no conflicts of interest related to this article.

Data availability. The data that support the findings of this study are available from the corresponding author upon reasonable request.

References

1. P. Fuchs, J. Seufert, J. Koeth, J. Semmel, S. Höfling, L. Worschech, and A. Forchel, "Widely tunable quantum cascade lasers with coupled cavities for gas detection," Appl. Phys. Lett. **97**(18), 181111 (2010).
2. L. Bizet, R. Vallon, B. Parvitte, M. Brun, G. Maisons, M. Carras, and V. Zeninar, "Multi-gas sensing with quantum cascade laser array in the mid-infrared region," Appl. Phys. B **123**(5), 145 (2017).
3. G. P. Luo, C. Peng, H. Q. Le, and S. S. Pei, "Grating-tuned external-cavity quantum-cascade semiconductor lasers," Appl. Phys. Lett. **78**(19), 2834–2836 (2001).
4. A. Hugi, R. Terazzi, Y. Bonetti, A. Wittmann, M. Fischer, M. Beck, J. Faist, and E. Gini, "External cavity quantum cascade laser tunable from 7.6 to 11.4 μm," Appl. Phys. Lett. **95**(6), 061103 (2009).
5. B. G. Lee, M. Belkin, C. Pflugl, L. Diehl, H. A. Zhang, R. M. Audet, J. MacArthur, D. Bour, S. Corzine, G. Hofler, and F. Capasso, "DFB quantum cascade laser arrays," IEEE J. Quantum Electron. **45**(5), 554–565 (2009).
6. B. G. Lee, H. A. Zhang, C. Pflugl, L. Diehl, M. Belkin, M. Fischer, A. Wittmann, J. Faist, and F. Capasso, "Broadband Distributed-Feedback Quantum Cascade Laser Array Operating From 8.0 to 9.8 μ m," IEEE Photonics Technol. Lett. **21**(13), 914–916 (2009).
7. E. Mujagić, C. Schwarzer, Y. Yao, J. Chen, C. Gmachl, and G. Strasser, "Two-dimensional broadband distributed-feedback quantum cascade laser arrays," Appl. Phys. Lett. **98**(14), 141101 (2011).
8. Y. Bidaux, A. Bismuto, C. Tardy, R. Terazzi, T. Gresch, S. Blaser, A. Muller, and J. Faist, "Extended and quasi-continuous tuning of quantum cascade lasers using superstructure gratings and integrated heaters," Appl. Phys. Lett. **107**(22), 221108 (2015).
9. M. Razeghi, W. J. Zhou, R. McClintock, D. H. Wu, and S. Slivken, "Progress in monolithic, broadband, widely tunable midinfrared quantum cascade lasers," Opt. Eng. **57**(01), 1 (2018).

10. W. Zhou, D. H. Wu, R. McClintock, S. Slivken, and M. Razeghi, "High performance monolithic, broadly tunable mid-infrared quantum cascade lasers," Optica **4**(10), 1228 (2017).

11. B. Meng, J. Tao, X. H. Li, Y. Q. Zeng, S. Wu, and Q. J. Wang, "Tunable single-mode slot waveguide quantum cascade lasers," Appl. Phys. Lett. **104**(20), 201106 (2014).

12. F. Smyth, E. Connolly, B. Roycroft, B. Corbett, P. Lambkin, and L. P. Barry, "Fast wavelength switching lasers using two-section slotted Fabry–Perot structures," IEEE Photonics Technol. Lett. **18**(20), 2105–2107 (2006).

13. R. Phelan, W. H. Guo, Q. Y. Lu, D. Byrne, B. Roycroft, P. Lambkin, B. Corbett, F. Smyth, L. P. Barry, B. Kelly, J. O. Gorman, and J. F. Donegan, "A novel two-section tunable discrete mode Fabry-Perot laser exhibiting nanosecond wavelength switching," IEEE J. Quantum Electron. **44**(4), 331–337 (2008).

14. D. C. Byrne, J. P. Engelstaedter, W. H. Guo, Q. Y. Lu, B. Corbett, B. Roycroft, J. O. Callaghan, F. H. Peters, and J. F. Donegan, "Discretely tunable semiconductor lasers suitable for photonic integration," IEEE J. Sel. Top. Quantum Electron. **15**(3), 482–487 (2009).

15. M. Nawrocka, Q. Y. Lu, W. H. Guo, A. Abdullaev, F. Bello, J. O'Callaghan, T. Cathcart, and J. F. Donegan, "Widely tunable six-section semiconductor laser based on etched slots," Opt. Express **22**(16), 18949 (2014).

16. M. J. Wallace, G. Jain, R. Mckenna, F. Bello, and J. F. Donegan, "Tuning behaviour of slotted vernier widely tunable lasers," Opt. Express **27**(12), 17122 (2019).

17. B. Meng, Y. Q. Zeng, G. Z. Liang, J. Tao, X. N. Hu, E. Rodriguez, and Q. J. Wang, "Broadly continuously tunable slot waveguide quantum cascade lasers based on a continuum-to-continuum active region design," Appl. Phys. Lett. **107**(11), 111110 (2015).

18. R. Maulini, M. Beck, J. Faist, and E. Gini, "Broadband tuning of external cavity bound-to-continuum quantum-cascade lasers," Appl. Phys. Lett. **84**(10), 1659–1661 (2004).

19. W. H. Guo, Q. Y. Lu, M. Nawrocka, A. Abdullaev, J. O'Callaghan, and J. F. Donegan, "Nine-channel wavelength tunable single mode laser array based on slots," Opt. Express **21**(8), 10215 (2013).

20. Q. Y. Lu, W. H. Guo, D. Byrne, and J. F. Donegan, "Design of slotted single-mode lasers suitable for photonic integration," IEEE Photonics Technol. Lett. **22**(11), 787–789 (2010).

21. M. J. Wallace, S. T. Naimi, G. Jain, R. McKenna, F. Bello, and J. F. Donegan, "Genetic algorithm optimization of high order surface etched grating tunable laser array," Opt. Express **28**(6), 8169 (2020).

22. M. McDermott, R. McKenna, C. Murphy, D. Mickus, H. Z. Weng, S. Naimi, Q. Y. Lu, W. H. Guo, M. Wallace, N. Abadía, and J. F. Donegan, "1.3 µm wavelength tunable single-mode laser arrays based on slots," Opt. Express **29**(10), 15802 (2021).

23. D. H. Wu and M. Razeghi, "High power, low divergent, substrate emitting quantum cascade ring laser in continuous wave operation," APL Materials **5**(3), 035505 (2017).

24. P. Rauter, S. Menzel, A. K. Goyal, B. Gökden, C. A. Wang, A. Sanchez, G. W. Turner, and F. Capasso, "Master-oscillator power-amplifier quantum cascade laser array," Appl. Phys. Lett. **101**(26), 261117 (2012).